Disruption of the Retinal Parafoveal Capillary Network in Type 2 Diabetes before the Onset of Diabetic Retinopathy

Johnny Tam,[1] *Kavita P. Dhamdhere,*[2] *Pavan Tiruveedhula,*[2] *Silvestre Manzanera,*[2] *Shirin Barez,*[2] *Marcus A. Bearse, Jr,*[2] *Anthony J. Adams,*[2] *and Austin Roorda*[1,2]

PURPOSE. To establish, using adaptive optics scanning laser ophthalmoscopy (AOSLO), that the retinal parafoveal capillary network is altered before the onset of diabetic retinopathy in adult patients with type 2 diabetes.

METHODS. AOSLO videos were acquired in the parafoveal region of one eye from control subjects and from patients with type 2 diabetes and no retinopathy. Detailed images of the parafoveal capillary network were generated with custom motion contrast enhancement algorithms. The combination of AOSLO images and videos enabled the simultaneous assessment of several features of the parafoveal capillary network. Arteriovenous (AV) channels were identified by finding the least tortuous capillary channels connecting terminal arterioles to postcapillary venules. Measures of capillary dropout and capillary hemodynamics were also quantified.

RESULTS. The average tortuosity of AV channels was 26% higher in patients with type 2 diabetes when compared with controls, even though there were no signs of diabetic retinopathy in any of the eyes that were assessed ($P < 0.05$). In addition, the metrics of capillary dropout showed small changes (between 3% and 7%), leukocyte speed 14% lower, and pulsatility 25% higher, but none of these differences was statistically significant.

CONCLUSIONS. It is often difficult to find consistent changes in the retinal microvasculature due to large intersubject variability. However, with a novel application of AOSLO imaging, it is possible to visualize parafoveal capillaries and identify AV channels noninvasively. AV channels are disrupted in type 2 diabetes, even before the onset of diabetic retinopathy. (*Invest Ophthalmol Vis Sci.* 2011;52:9257–9266) DOI:10.1167/iovs.11-8481

Type 2 diabetes is a disease that produces gradual changes in many different systems throughout the body, including the retinal parafoveal capillary network. Retinal capillary beds are more vulnerable than others in the body because of the metabolic demands imposed by the surrounding retinal tissue. In the eye, type 2 diabetes can cause diabetic retinopathy (DR). The prevalence of DR has been reported to be 35% in patients who have had diabetes for 12 years.[1] The earliest clinical signs of DR are microaneurysms (small outpouchings of the capillaries) and dot intraretinal hemorrhages. Although the natural progression of DR from these signs into the late stages has been well characterized, the early microvascular changes that precede DR have not been established, since it is very difficult to assess live human retinal capillaries, due to their small size and low optical contrast. Fluorescein angiography (FA), an invasive procedure and the gold standard for visualizing human retinal capillaries, is not performed under normal situations on patients with type 2 diabetes and no DR, since there is little clinical justification for performing an FA at this stage. Also, as with any invasive procedure, there is a small risk of adverse side effects.[2] Moreover, there are very few animal models that can be used to investigate the capillary network before the onset of DR[3] and even fewer that can be used to investigate both type 2 diabetes and DR.[4]

Capillary networks are complex. In a terminal capillary bed, there are arterioles, capillaries, and venules. In general, capillaries can be classified into two categories: thoroughfare channels and exchange capillaries. Thoroughfare channels can be identified as those capillaries that, under normal conditions, provide the most direct path for blood cells from terminal arterioles to postcapillary venules[5–7]; all remaining neighboring capillaries are exchange capillaries. Assessment of capillary hemodynamics without consideration of the type of capillary or the proximity of the capillary to a thoroughfare channel can lead to misinterpretation of results. Although there have been previous studies that have investigated capillary hemodynamics in live human retinal capillaries,[8,9] the measurements were performed on isolated capillary segments without taking into consideration the relationship of the capillary to the surrounding network.

Assessment of the human parafoveal capillary network is commonly performed with a macroscopic metric such as foveal avascular zone (FAZ) size and shape[10–14] or perifoveal intercapillary area.[13] Although there is a relationship between FAZ size and DR severity, there is large intersubject variability; the average FAZ area of nondiseased eyes has been reported by three different studies as 0.152 ± 0.086,[12] 0.367 ± 0.090,[13] and 0.405 ± 0.559[11] (mean square millimeters $\pm$ SD, as measured using FA). Thus, the large intersubject variability makes it difficult to detect changes, especially in the early stages of the disease. Moreover, these metrics mask several unique topologic features of the parafoveal capillary network. First, vessels are oriented in a specific manner. Capillaries are preferentially oriented circumferentially, while arterioles and venules are preferentially oriented radially; arterioles and

venules are also arranged in an interdigitating manner (i.e., as one moves circumferentially around the FAZ, one encounters an arteriole, then a venule, followed by an arteriole, and another venule, and so on).[15,16] There are, on average, 2.9 terminal arterioles that directly supply the capillaries at the edge of the FAZ.[15] Second, there is a variation in capillary density in the circumferential direction. The capillary density is slightly increased near venules and slightly decreased near arterioles,[15–17] because of the small capillary-free zone that surrounds arterioles. However, this effect is diminished as one approaches the edge of the FAZ.[16] Finally, there is also a variation in capillary density in the radial direction. The capillaries form a planar, single-layered structure immediately outside of the FAZ. As one moves radially outward, a deeper capillary layer begins, although this deeper layer is sparser than the superficial layer.[16] Consequently, in the parafoveal capillary network, capillary density is more dependent on proximity from the edge of the FAZ than on eccentricity. Any of these topologic features could become affected in DR with little consequence on a macroscopic metric of capillary density. Thus, there is a need for more sensitive imaging biomarkers to characterize DR.

DR is a heterogeneous disease. In the early stages, most vascular lesions are focal, affecting only a small subset of capillaries. This is not surprising, given that the topography of the capillary network is highly heterogeneous. However, it makes it difficult to define quantitative metrics when assessing early signs of capillary disruption and blood flow, since normal regions of the microvasculature are likely to dominate focal abnormal regions when using any given metric. We hypothesize that there are specific capillary channels within the parafoveal capillary network which are affected in DR. Disruption of such channels would lead to a change in the distribution of blood flow through the network, which could lead to the development of clinical signs of DR.

Recently, we have developed noninvasive methods to visualize and assess the human parafoveal capillary network,[18,19] with the ability to assess hemodynamics of specific capillaries in relation to the surrounding capillary network,[7] using an adaptive optics scanning laser ophthalmoscope (AOSLO).[20,21] In this article, we use a novel application of the AOSLO to determine the relationship between capillary channels, capillary network topology, and capillary hemodynamics in patients with type 2 diabetes and no DR. The detailed images generated using the AOSLO may enable us to detect changes in individual capillaries that were previously undetectable.

METHODS

Research procedures adhered to the tenets of the Declaration of Helsinki. After a detailed explanation of procedures, written informed consent was obtained from all participants. The research protocols were approved by the University of California, Berkeley Committee for Protection of Human Subjects.

Subjects

The study recruited 30 human subjects: 15 adult patients with a diagnosis of type 2 diabetes for at least 5 years, with no DR in at least one eye (T2DM_NoDR), and 15 adult age-matched control subjects with no history of diabetes (control). Exclusion criteria were prior ocular surgery (including refractive surgeries), cataract or media opacities, and ocular diseases not associated with diabetes (including any retinopathy). Patients who were pregnant or nursing (lactating) were also excluded.

AOSLO Imaging

One eye from each subject was selected for imaging. In a few subjects, only one eye satisfied all inclusion criteria. If both eyes satisfied all inclusion criteria, then the eye with the lower spherical equivalent refractive error was selected for imaging. The selected eye was dilated (2.5% phenylephrine hydrochloride, 1% tropicamide).

Images of the parafoveal capillary network were generated noninvasively, without the injection of contrast agent, as described previously.[7,18] Briefly, overlapping AOSLO videos were acquired in the parafoveal region (1.8° field size, 40 seconds, and 60 Hz). The subject's pulse was measured using a photoplethysmograph (MED Associates, Inc., St. Albans, VT) and simultaneously recorded in a data file during acquisition of all videos. Custom motion–contrast enhancement algorithms were applied offline to generate capillary perfusion images from each of the acquired AOSLO videos, and the resulting capillary perfusion images were assembled to generate a montage of the parafoveal capillary network, showing the FAZ and surrounding parafoveal capillaries (Fig. 1).

AOSLO images of the parafoveal capillary network were successfully generated in 12 of 15 T2DM_NoDR subjects and 12 of 15 control subjects. The overall success rate for AOSLO imaging was 24 (80%) of 30 subjects. The proportion of subjects undergoing conventional FA who had images of sufficient quality for the delineation of individual parafoveal capillaries was 13 (76%) of 17 in a prior study.[13] The success rate of delineating the FAZ using oral FA combined with confocal scanning laser ophthalmoscopy was 16 (47%) of 34.[22] Notably, AOSLO images are generated with minimal risk considering the noninvasive nature of the method. Images of perfused capillaries were used to compare the two groups for qualitative differences. Specifically, we examined AOSLO images for subclinical capillary peculiarities, such as capillary bends and possible precursors to microaneurysms, as well as possible breakdown of the topologic organization of the capillary network.

Clinical Assessment

Medical History. All subjects provided a medical history to verify inclusion and exclusion criteria as outlined above. One control subject was excluded because of a diagnosis of age-related macular degeneration (AMD). For the T2DM_NoDR subjects, hemoglobin A1c (HbA1c) levels were measured, and a slit lamp examination was performed to verify the absence of cataract before AOSLO imaging.

Biometry Measurements. Axial length, anterior chamber depth, and corneal curvature were measured and used to make accurate conversions from visual angle to distance, as described elsewhere[23] (IOL Master; Carl Zeiss Meditec Inc., Dublin, CA).

Fundus Photography and Grading. A digital fundus camera was used to acquire 45° fundus photographs near the posterior pole for all subjects (Visucam Pro NM; Carl Zeiss Meditec Inc., Dublin, CA). For the T2DM_NoDR subjects, two additional photographs were taken (nasal and temporal to the fovea), and the three overlapping color fundus photographs were evaluated by a retina specialist to determine whether there were signs of any retinopathy. Photographs were evaluated off site with no subject-identifying information and no information about the subject's medical history. They were assigned a grading of no retinopathy, mild nonproliferative diabetic retinopathy (NPDR), moderate NPDR, severe NPDR, or proliferative diabetic retinopathy (PDR). In addition, macular edema and any other signs of retinopathy not related to diabetes were noted.

The retina specialist assigned a grading of no retinopathy to all T2DM_NoDR eyes that were selected for AOSLO imaging. Three of the T2DM_NoDR subjects were assigned a grading of mild NPDR in the contralateral eye. After the subject from the control group who presented with AMD (as described above) was excluded, AOSLO images of the parafoveal capillary network from 12 T2DM_NoDR subjects and 11 control subjects were generated and used for comparison. The mean and SD of the ages were 55.5 ± 7.6 years for the T2DM_NoDR subjects and 52.2 ± 10.6 years for the control subjects. Detailed information about these subjects is presented in Table 1. There was a difference in the composition of the ethnicities between the two groups (ethnicity was neither an inclusion criteria nor an exclusion criteria, and thus no
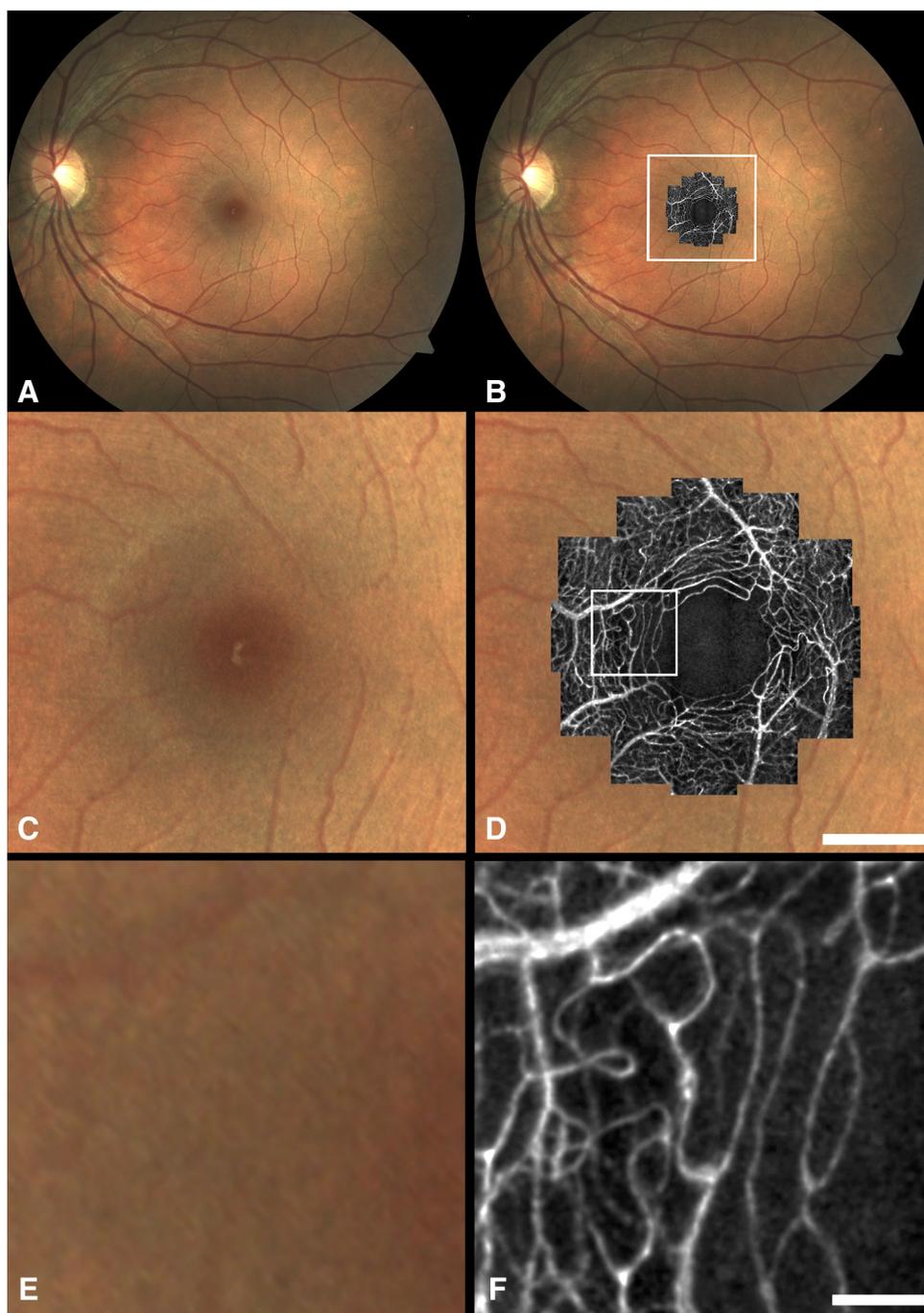
FIGURE 1. Example of AOSLO imaging for one control subject. In this example, overlapping videos were taken in 21 different locations on the retina, processed to generate capillary images, and then compiled to generate a montage of the parafoveal capillary network. (**A**, **B**) A 45° fundus photograph, with and without AOSLO images. (**C**, **D**) Higher magnification of the *white box* in (**B**), showing a portion of the fundus photograph, with and without AOSLO images. (**E**, **F**) Higher magnification of the *white box* in (**D**), showing the fundus photograph, with and without one AOSLO image generated from a single video. Scale bar: (**C**, **D**) 500 μm; (**E**, **F**) 100 μm.

attempt was made to select for ethnicity during subject recruitment). Although the prevalence of diabetes is higher in the Mexican-American population, the prevalence of DR is similar when compared to a Caucasian population.[24] Thus far, there have been no major studies that have shown any ethnic differences in the parafoveal capillary network near the FAZ.

Identification of Arteriovenous Channels

We identified AV channels (defined here as the simplest, most direct capillary paths connecting arteries to veins) and calculated tortuosity. The concept of AV channels is based on thoroughfare channels.[5,6] In the absence of anastomoses (bypass vessels between macular arterioles or venules), as has been shown in the human retina,[16] thoroughfare channels can be identified as the simplest, most direct paths connect-

ing arterioles to venules. We used the following steps to identify AV channels (Fig. 2).

First, we identified the locations of arterioles and venules. The largest vessels in the AOSLO images were matched to the smallest vessels in the color fundus photographs. Locations of arterioles and venules could be identified by following arteries and veins directly into the AOSLO images. Second, we drew paths to represent candidate AV channels, starting at an arteriole and ending at a venule, applying a simple rule at each branch point. At each branch point, we selected the branch with the smallest branch angle, where branch angle was defined as the angle between the centerline of the vessel upstream of the branch point, and the centerline of the branch. If both branch angles were similar, then both paths were selected. By proceeding in this manner for all arterioles and branch points, we generated a set of candidate AV channels. Finally, we identified the three least tortuous

TABLE 1. Subject Characteristics

Subject*	Sex	Age	Eye	Ethnicity	Duration (y)	HbA1c
C2	F	33	OS	Caucasian	N/A	N/A
C3	M	37	OD	Caucasian	N/A	N/A
C4	F	59	OS	Caucasian	N/A	N/A
C5	F	53	OD	Caucasian	N/A	N/A
C6	F	52	OD	Caucasian	N/A	N/A
C7	M	51	OD	Caucasian	N/A	N/A
C9	M	63	OS	Black	N/A	N/A
C11	M	55	OD	Caucasian	N/A	N/A
C12	M	70	OD	Caucasian	N/A	N/A
C14	M	47	OS	Caucasian	N/A	N/A
C15	M	54	OS	Caucasian	N/A	N/A
D1	M	38	OD†	Asian	14	6.1
D3	M	56	OD	Native American	6	13.1
D6	F	45	OD†	Hispanic	12	7.2
D7	M	57	OD	Caucasian	8	7.5
D8	F	53	OS	Hispanic	10	7.4
D9	F	63	OS	Hispanic	10	6.8
D10	M	57	OD	Caucasian	8	6.6
D11	M	64	OS	Caucasian	8	7.3
D12	F	53	OS	Hispanic	5	7.8
D13	F	63	OS	Caucasian	12	6.5
D14	F	63	OD†	Hispanic	10	7.3
D15	F	54	OS	Hispanic	14	7.8

* C2 to C15 are control subjects; D1 to D15 are T2DM_NoDR subjects.
† Subject presented with mild NPDR in the contralateral eye.

AV channels. There are, on average, approximately three terminal arterioles that feed the capillaries immediately outside of the FAZ[16]; thus, we expected to find three AV channels.

To quantify tortuosity, we selected a metric that emphasizes areas of high curvature and de-emphasizes areas of low curvature, noting that the curvature of smaller vessels is greater than larger vessels.[25] This definition of tortuosity is fairly consistent with the clinical notion of tortuosity[25]:

$$\text{Tortuosity} = \frac{\text{total squared curvature of the line}}{\text{length of the line}} = \frac{\text{TSC}}{\text{L}}. \quad (1)$$

To minimize the effect of the discrete nature of pixel representation, we used a sliding least-squares polynomial fitting scheme to calculate the curvature. To calculate the curvature at each point along the channel, we extracted a 20-μm segment centered around the point and calculated the least-squares cubic polynomial fit for that segment. We used the polynomial fit to calculate the curvature, based on taking the first and second derivatives of the polynomial, as described previously.[25]

We identified the three least tortuous AV channels and calculated the average tortuosity of these three channels. Not all AOSLO images could be analyzed for AV channel tortuosity, because there were variations in data quality both within and across subjects. We attempted to quantify AV channel tortuosity only in the subjects whose FAZs could be delineated using the AOSLO. Thus, the quality of the AOSLO images was sufficient to enable AV channel tortuosity measurements in 11 of 11 control subjects and 11 of 12 T2DM_NoDR subjects.

Macroscopic Measures of Capillary Dropout

We calculated three measures of capillary dropout: FAZ size, FAZ shape, and capillary density. We attempted to quantify measures only in those subjects whose FAZs could be delineated using the AOSLO. Because of variations in the appearance of the FAZ, the number of overlapping AOSLO videos required to fully visualize the FAZ ranged from 9 to 21 videos. Since there were variations in the quality of videos both within and across subjects, sometimes it was not possible to quantify a specific metric across all subjects. However, in all cases, metrics were quantified in as many subjects as possible.

FAZ Size. The borders of the FAZs were extracted using a semi-automated algorithm, as described previously.[18] We identified the FAZ as the largest avascular zone near the fovea. The area of the extracted region was quantified in square pixels and then converted to square millimeters using a model eye parameterized by the biometry measurements from each subject. The effective diameter of the FAZ was calculated as the diameter of the circle with equal area:

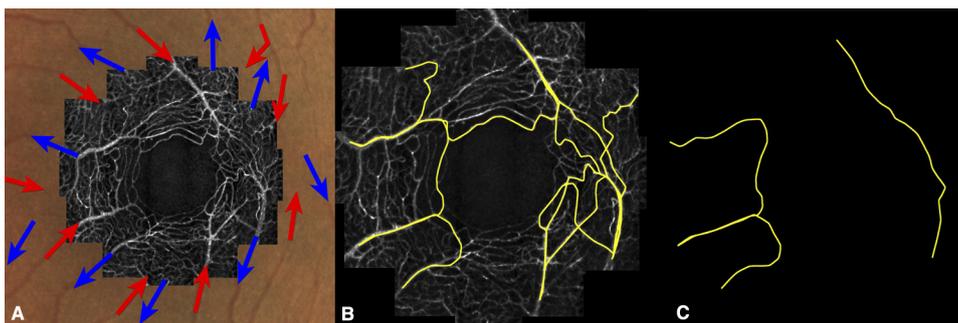$$\text{Effective diameter} = 2\sqrt{\frac{\text{area}}{\pi}}. \quad (2)$$

FIGURE 2. Identification of AV channels on AOSLO images. The steps are: (**A**) identify locations of arterioles (*red*) and venules (*blue*), (**B**) identify candidate AV channels satisfying the branch selection rule, and (**C**) select the three least tortuous AV channels.

The quality of the AOSLO images was sufficient to enable quantification of the FAZ size in 11 of 11 control subjects and 12 of 12 T2DM_NoDR subjects.

FAZ Shape. We measured the shape of the FAZ using the following acircularity metric:

$$\text{Acircularity} = \frac{\text{perimeter of the FAZ}}{\text{perimeter of the circle with equal area}}. \quad (3)$$

A perfectly circular FAZ has an acircularity equal to 1. Deviations from a circular shape increase the value of this acircularity metric.

The quality of the combined AOSLO images was sufficient to enable FAZ shape measurements in 11 of 11 control subjects and 9 of 12 T2DM_NoDR subjects.

Capillary Density. The centerlines of all vessels in a region of interest (ROI) within 0.15° of the edge of the FAZ were extracted using a semiautomated extraction process, as described previously.[18] The inner border of the ROI was defined as the edge of the FAZ, and the outer border was defined as the contour spaced 0.15° from the edge of the FAZ. In the parafovea, capillary density increases in a discontinuous manner, from 0 inside to FAZ to an intermediate value in the region of single-layered capillaries, with subsequent increases corresponding to the introduction of additional capillary layers. The eccentricities at which the additional capillary layers begin depend largely on the size of the FAZ; moreover, with an irregularly shaped FAZ, the transition may occur at different eccentricities depending on the direction (e.g., superior versus inferior). Therefore, to minimize confounding factors, we elected to use the ROI defined by the actual shape of the FAZ to capture the approximate zone where the capillary network is single-layered. We defined the capillary density metric as:

$$\text{Capillary density} = \frac{\text{total length of all extracted capillaries}}{\text{area of the ROI}} = \frac{L}{A}. \quad (4)$$

The quality of the AOSLO images was sufficient to enable capillary density measurements in 8 of 11 control subjects and 9 of 12 T2DM_NoDR subjects.

Capillary Hemodynamics

We calculated two measures of capillary hemodynamics: leukocyte speed and pulsatility index. As for the previous metrics, we attempted to quantify hemodynamics only on those subjects whose FAZs could be delineated with the AOSLO.

Leukocyte Speed. We quantified the speed of leukocytes through selected AV channels. Under normal physiological conditions, there is considerable variation in the distribution of leukocytes across the parafoveal capillary network.[7] Some AV channels contained many leukocytes, whereas others did not. We identified the least tortuous AV channel that also contained many leukocytes and measured the speed of all leukocytes that could be clearly identified in the corresponding 40-second AOSLO video. The speed of each leukocyte was quantified directly, incorporating corrections for raster scanning and eye motion, as described previously.[19] We then calculated the average leukocyte speed by plotting leukocyte speed versus relative cardiac cycle, dividing the cardiac cycle into five bins, calculating the average speed of each bin, and then taking the average speed of the five bins. Relative cardiac cycle was determined from the subject's pulse data, which was simultaneously recorded during video acquisition. Thus, leukocyte speeds were normalized for variations due to the cardiac cycle.

The quality of the AOSLO videos was sufficient to enable leukocyte speed measurements in 8 of 11 control subjects and 7 of 12 T2DM_NoDR subjects.

Pulsatility Index. We calculated the pulsatility index (PI) for leukocytes by using a method described previously.[7] Briefly, leukocyte speeds were plotted versus relative cardiac cycle, and divided into five bins. We defined V_{max} as the bin with highest average speed, V_{min} as the bin with the lowest speed, and V_{mean} as the average speed of all five bins. PI was calculated as:

$$\text{PI} = \frac{V_{max} - V_{min}}{V_{mean}}. \quad (5)$$

We calculated PI only when there were at least two leukocytes identified in each bin. Applying this criteria, we calculated PI in 7 of 11 control subjects and 5 of 12 T2DM_NoDR subjects.
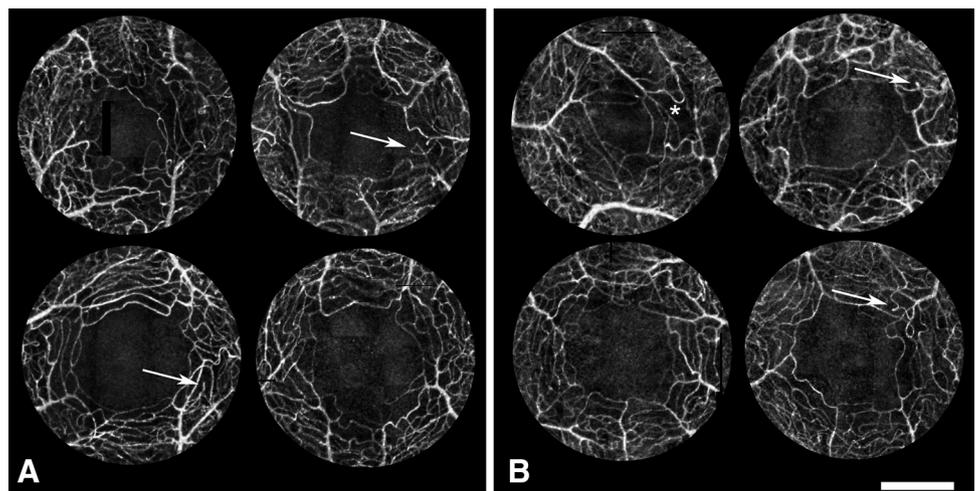
Statistical Analysis

We compared the two groups using two-tailed unpooled *t*-tests with a significance level of 0.05.

RESULTS

In general, there were no obvious homogeneous differences that could be observed between the T2DM_NoDR and control groups (Fig. 3). The interdigitating arteriole and venule organization was maintained in all images. It appeared that there were areas of focal capillary disruption, notably around areas of capillary bend formation. Interestingly, capillary bends were present in both groups, suggesting that some aspects of capillary disruption may be present, even in healthy subjects (Fig. 4). There were also objects that may be precursors to microaneurysms present in both groups; such

FIGURE 3. Examples of parafoveal capillary montages generated using custom motion contrast enhancement algorithms. Higher intensities denote areas of greater intensity fluctuations due to blood flow as seen on unprocessed AOSLO videos. Subtle variations in intensity in noncapillary areas are artifacts due to the use of multiple overlapping videos. There were no obvious qualitative differences in appearance between the two groups. Shown are examples: (**A**) four control subjects and (**B**) four T2DM_NoDR subjects. *Arrows*: denote examples of peculiar capillary bends (shown in more detail in Fig. 4). (**B**, ✱) A rather large, avascular region outside of the FAZ, which may be indicative of early capillary dropout. Scale bar, 500 μm.
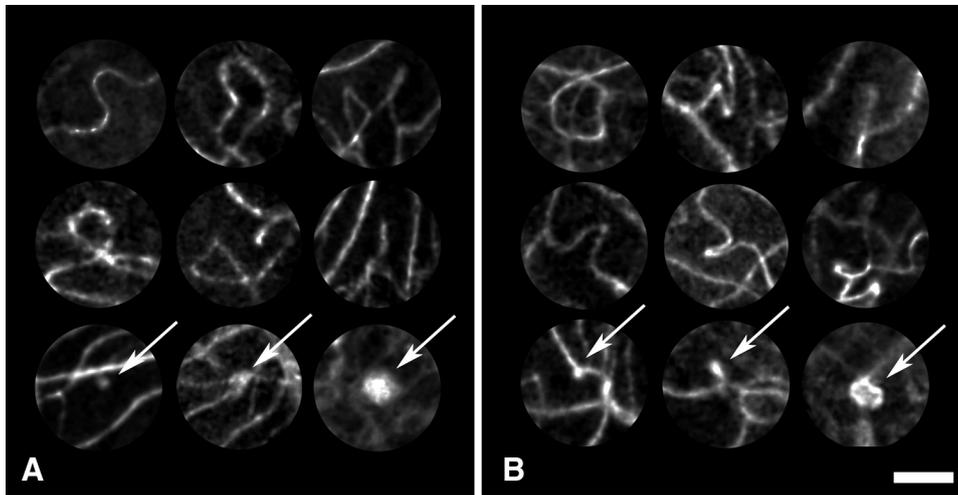
Figure 4. Examples of capillary abnormalities in (**A**) control and (**B**) T2DM_NoDR subjects. There were capillary bends and dead-end capillaries present in both groups (*top two rows*), as well as objects of various sizes that were similar in appearance to microaneurysms (*bottom row, arrows*), despite the absence of microaneurysms on color fundus photographs. Scale bar, 100 μm.

objects were not clinically identified as microaneurysms based on fundus photography. When identifying such objects, it should be noted that interpretation of AOSLO images is different from interpretation of FA images, as sources of hyper- and hypointensity are different; in FA, intensity is a measure of fluorescein dye accumulation and may be indicative of leakage; in AOSLO images, intensity is a measure of high relative flow, with no information about leakage.

AV channels were identified, extracted, and quantified for tortuosity (Fig. 5). Extracted FAZs and capillaries are shown (Figs. 6, 7).

Statistical Analysis

The average AV channel tortuosity was 26% higher in T2DM_NoDR subjects than in the controls ($P < 0.05$). There were no statistically significant differences in capillary dropout or capillary hemodynamics (Fig. 8). Comparing T2DM_NoDR to controls, the average FAZ size was 7.4% higher, FAZ shape 3.4% higher, capillary density 3.7% lower, leukocyte speed 14.4% lower, and pulsatility index 25% higher. It was difficult to assess whether all variables followed a normal distribution, particularly in the case of FAZ shape, where there was one

outlier. Therefore, we also performed Wilcoxon rank sum tests, which confirmed that AV channel tortuosity was significantly higher ($P < 0.05$), with none of the other metrics testing as significantly different.

Discussion

We have shown, without fluorescein angiography, that AV channels in the human retinal parafoveal capillary network are disrupted in the early stages of type 2 diabetes, even before any signs of DR. Since most capillaries are exchange capillaries, with only a select few comprising the AV channels, it is relatively difficult to detect this change when using macroscopic metrics to assess the parafoveal capillary network.

Based on the results of this study, we propose a novel hypothesis for the development of clinical microvascular changes (Fig. 9). Unlike prior studies, this model links microvascular changes and hemodynamics to account for clinical signs.

We hypothesize that there is an ongoing cycle of AV channel disruption, which propagates with a redistribution of leukocytes out of AV channels and into exchange capillaries. A redistribution of blood flow before the onset of DR has been reported in a streptozotocin rat model of diabetes.[3] Initially, with incremental changes in tortuosity, existing AV channels are likely to be replaced by new AV channels, which would be the next, least tortuous path connecting arterioles to venules. However, replacement AV channels would likely include some exchange capillaries, which may not be suitable for increased leukocyte traffic. Specifically, the passage time for leukocytes through exchange capillaries is likely to be much higher than for leukocytes through AV channels. This would lead to an overall accumulation of leukocytes in the network, consistent with previous findings.[26] These leukocytes inside exchange capillaries may lead to focal capillary dropout, for which many leukocyte-based mechanisms have been proposed,[27] which may be triggered by a decrease in the deformability and increase in activation of diabetic polymorphonuclear leukocytes.[28,29] As the cycle of AV channel disruption continues, one can imagine that there could be two points of no return: first, when all AV channels have been replaced by exchange capillaries, and second, due to progressive disruption, when there are finally no longer any more viable replacement AV channels.

This cycle could lead to clinical signs of DR, with endothelial cell remodeling resulting in the formation of microaneurysms and intraretinal microvascular abnormalities. If leuko-
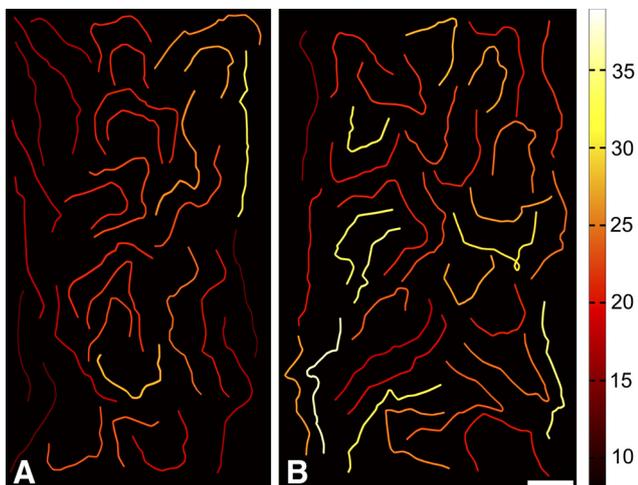

Figure 5. The three least tortuous AV channels from the (**A**) control and (**B**) T2DM_NoDR subjects. The capillary segments are arranged to best fill the space in each panel of the figure. The color map shows the range of tortuosities (arbitrary units, generated by calculating TSC/L · 10^5; equation 1). Scale bar, 500 μm.
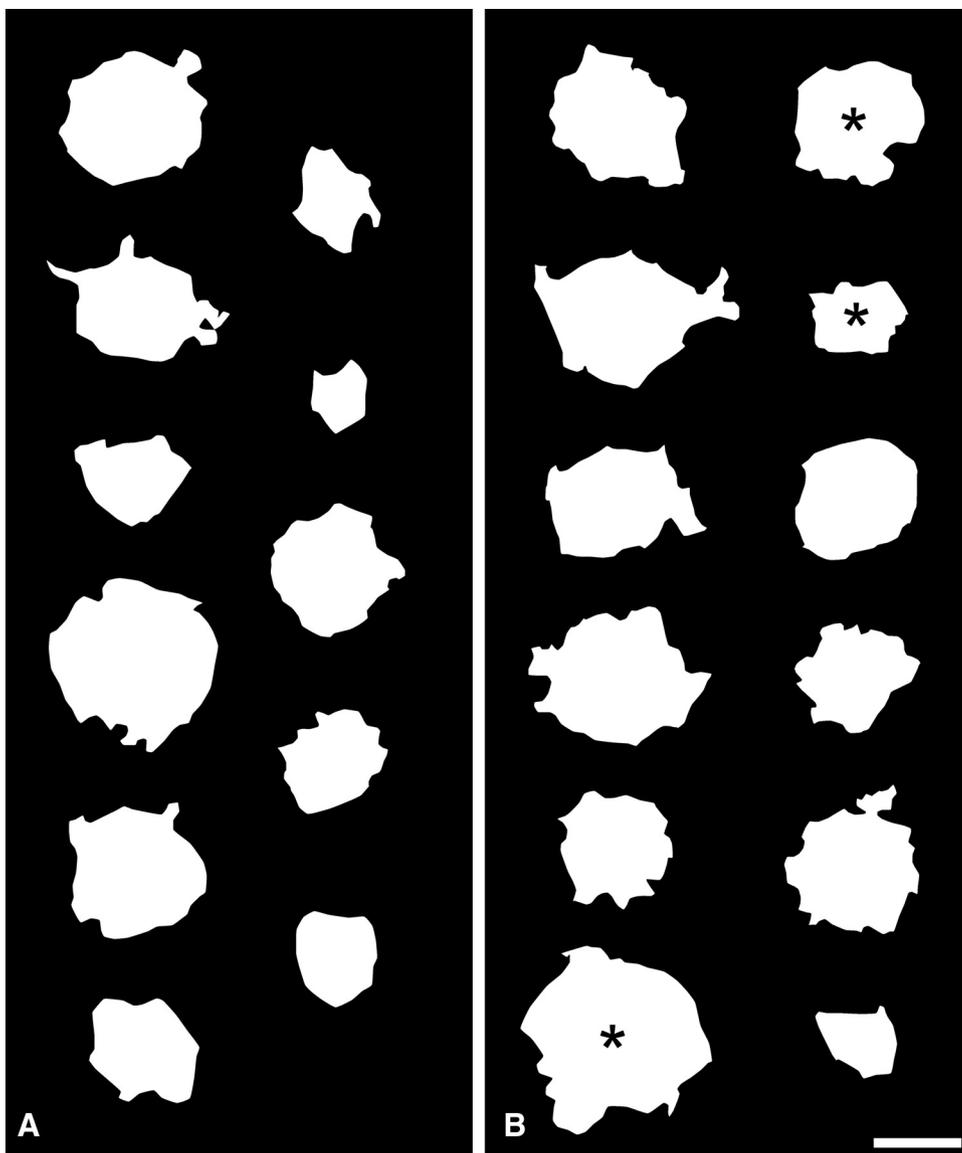
FIGURE 6. Extracted FAZs for (**A**) control and (**B**) T2DM_NoDR subjects. Three FAZs could not be extracted due to poor data quality. Of the extracted FAZs, three FAZs were not used for quantification of FAZ shape because of poor quality data in one or more videos showing the edge of the FAZ (✱). For these FAZs, the extracted FAZ was estimated from the AOSLO image and quantified for size but not shape. Scale bar, 500 μm.

cytes were to accumulate inside microaneurysms, as has been qualitatively observed,[26,30] then this could lead to the subsequent disappearance of the affected microaneurysm. This accumulation of leukocytes inside microaneurysms would be aided by any redistribution of leukocytes resulting from AV channel disruption. Simultaneously, since leukocytes have such a dominant role in determining the flow mechanics in capillaries, disruption of the tissue homeostasis may lead to neural damage or formation of cotton wool spots. Therefore, disruption of AV channels could lead to the formation of clinically observed changes.

There are several potential explanations for why AV channel tortuosity is higher in the T2DM_NoDR group. First, it is possible that the increase is due to endothelial cell proliferation. However, given that our results occur before the formation of clinically identifiable microaneurysms (a sign of endothelial cell proliferation), it is unlikely that the increase in tortuosity can be attributed to endothelial cell proliferation alone. Second, it is possible that a flow parameter such as increased intramural pressure could contribute to an increase in tortuosity, as has been modeled using 7.9-mm diameter latex tubing.[31] However, it is unclear whether the mechanisms for increased tortuosity of larger vessels can be applied to capillaries, since capillaries are by nature more tortuous than larger vessels. Although it is tempting to apply existing mechanisms for increases in vessel tortuosity, it is important to keep in mind that our definition of AV channel tortuosity is based on finding the least tortuous paths. Hence, a higher AV channel tortuosity implies that the set of least tortuous paths is higher, but does not necessarily imply that the tortuosity of any one capillary segment has increased. Given these considerations, along with our hypothesis (Fig. 9), a higher AV channel tortuosity in patients without retinopathy may simply be the result of the progressive loss of key capillary segments.

Our results are consistent with previous studies that have investigated capillary dropout, which is a hallmark of NPDR. There are several methods to quantitatively assess capillary dropout. The most intuitive method is to quantify the size of the FAZ, with a larger FAZ corresponding to capillary dropout in the parafovea. Although some studies have found statistically significant increases in FAZ size in NPDR,[11,12] data from other studies show increases only in the later stages,[13,14] most likely because of the large intersubject variability in FAZ size. There is also some evidence that the FAZ becomes more acircular in DR, with greater effects on the perimeter than on the size.[10,12] Our measurements of FAZ size and shape are consistent with
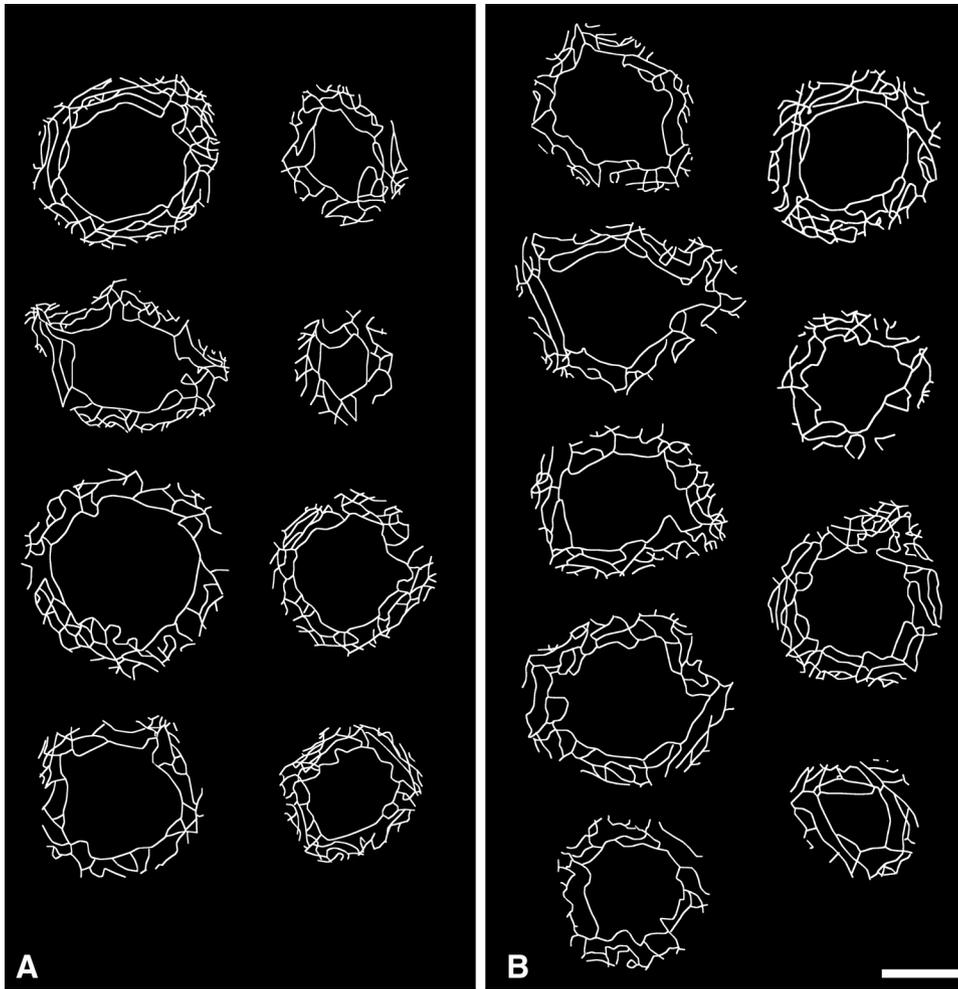
FIGURE 7. Extracted capillaries for (**A**) control and (**B**) T2DM_NoDR subjects. Some subjects could not be analyzed because of data quality in one or more portions within the ROI. Scale bar, 500 μm.

the numbers reported in these studies, falling between the numbers reported for normal and diabetic FAZs. Finally, our capillary density metric is similar to perifoveal intercapillary area, which has been found to increase in NPDR,[9,13] with the change likely to occur between mild NPDR and moderate NPDR.[13] These studies and the data from our study suggest that macroscopic capillary dropout is a gradual process that probably occurs only after the manifestation of clinical signs of DR.

There have been many studies of blood flow in DR. However, results are potentially confounded by differences in measurement location (e.g., arteriole, venule, or capillary; papillary, macular; retina, and choroid), disease severity (e.g., NPDR

and PDR), disease type (e.g., types 1 and 2), object of measurement (e.g., erythrocyte, leukocyte, and plasma bolus), or even disease model (e.g., rat, monkey and human). Considering only results from human subjects, it appears that blood flow in arteries and veins is decreased before the onset of DR[32-34] and increased during NPDR.[34-37] Perifoveal capillary velocity was found to be decreased in patients with diabetes,[9] consistent with the data in this study; however, papillomacular capillary blood flow was found to be increased in patients with type 2 diabetes but no DR,[8] suggesting that changes in the blood flow are heterogeneous. Finally, studies investigating the pulsatility of blood in choroidal vessels have found increases in pulsatility
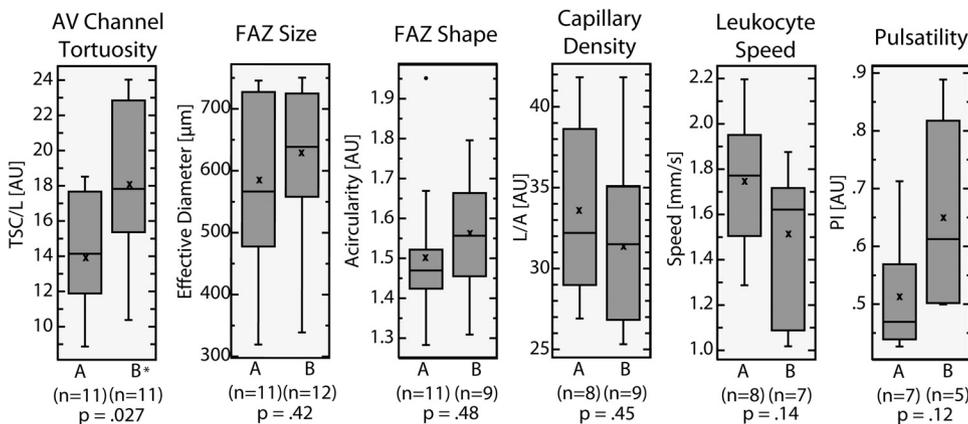

FIGURE 8. Results from statistical analyses, for control (**A**) and T2DM_NoDR (**B**) groups. AV channel tortuosity was significantly higher in the T2DM_NoDR group compared to the control group ($P < 0.05$). For FAZ shape, which had one outlier, a Wilcoxon rank sum test confirmed that the difference between groups was not statistically significant ($P = 0.26$).
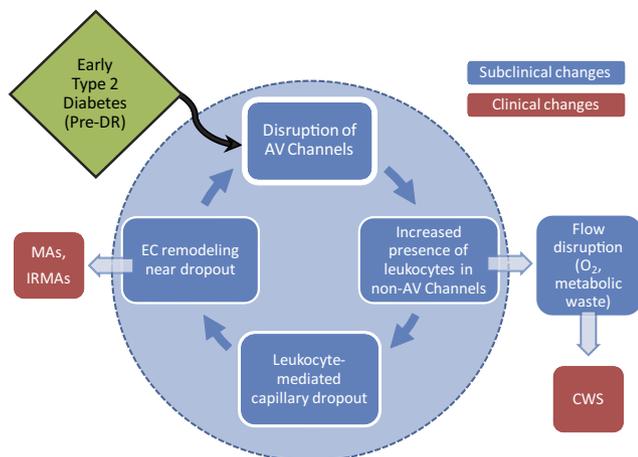
FIGURE 9. The proposed mechanism for progression from AV channel disruption to NPDR. EC, endothelial cell; MAs, microaneurysms; IRMAs, intraretinal microvascular abnormalities; CWS, cotton wool spots.

in the later stages of DR (severe NPDR, PDR),[38,39] but the results are inconsistent in the earlier stages, with decreases,[38] no change,[39] and increases[40] shown. In our study, leukocyte speed was 14% lower and the pulsatility index 25% higher. We identified capillary segments using AV channels to perform leukocyte speed measurements in the same corresponding location of the parafoveal capillary network in all subjects; furthermore, measured speeds were normalized for the cardiac cycle. The average heart rate, which was simultaneously recorded during the acquisition of every AOSLO video was similar in both groups (66.4 ± 11.7 for T2DM_NoDR and 64.7 ± 9.4 for controls, reported as mean beats per minute ± SD). Increased AV channel tortuosity is consistent with decreased leukocyte speed, since leukocytes must deform to travel through small capillaries in single file,[41] and any increase in tortuosity is likely to require additional deformations for leukocyte passage. In addition, the decreased leukocyte speed is consistent with the increased rigidity of diabetic leukocytes.[42] Although the results of statistical testing for these hemodynamic measures were not significant (i.e., inconclusive), such metrics may still be of clinical importance.

There are several limitations to this study.

First, the sample sizes of the control and T2DM_NoDR groups are small. Because of the small sample size, it was not meaningful to examine correlations with variables such as HbA1c, disease duration, or age. The age range in this study was narrow, as it was predetermined mostly by the inclusion criteria of type 2 diabetes with no DR, and at least 5 years' disease duration; by 15 years' duration, nearly 80% of type 2 diabetes patients have signs of DR.[43] Despite the small sample size, AV channel tortuosity was significantly different when comparing patients with type 2 diabetes and controls, suggesting that this metric is highly sensitive. In this study, we selected the three least tortuous channels. To explore the robustness of this metric, we also compared the least tortuous channel, as well as the average of the two least, four least, and five least tortuous channels, and found statistically significant differences in all cases. However, larger studies should be undertaken to validate our findings.

Second, the ethnicity is markedly different between the two groups. Although there are no studies to suggest that the parafoveal capillaries are different with respect to ethnicity, it is possible that changes may be due to ethnicity. We did not find changes in the macroscopic measures of capillary dropout, which supports our assumption that there are no significant ethnic differences.

Finally, the process of AOSLO imaging combined with video and image analysis is time-consuming and requires specialized equipment that is not yet commercially available. In this study, AOSLO imaging for one eye from each subject required approximately 2.5 hours, followed by approximately 20 hours of offline processing per eye to generate images of parafoveal capillaries and to quantify the metrics described in this study. However, these methods are not yet optimized, as nearly every step utilizes custom hardware and software. Future optimization and automation of imaging and processing will certainly result in significant improvements in speed.

In the future, studies should be performed to validate the AV channel tortuosity metric, perhaps by examining high-quality FAs to evaluate AV channel tortuosity in NPDR and PDR. Results from this study are important for planning future studies. As examples, our results suggest that approximately 180 subjects would be needed to achieve significance for a change in FAZ shape (when including the outlier), 160 subjects for a change in FAZ diameter, 120 subjects for capillary density, and approximately 30 subjects for leukocyte speed or pulsatility index (assuming a two-sided *t*-test, significance level 0.05, and power level 0.80).

In conclusion, we demonstrate a unique method to noninvasively assess retinal capillaries and leukocytes in patients with type 2 diabetes and no DR. Although there are now several methods for noninvasively visualizing capillaries in humans,[44–46] the system of imaging and analysis described in this article is unique in that capillaries and leukocytes can be analyzed from the same dataset. Furthermore, we offer a "causative" model that links microvascular changes and blood flow to clinical signs of DR (Fig. 9).

These new methods may be useful for assessing the microcirculation in other diseases, particularly as advances in technology reduce the time commitment for analysis and allow for larger study populations. This application may find the most use in cases when FA is not performed (for whatever clinical reason), or for establishing a normal database of parafoveal capillaries, since our data suggests that subclinical capillary peculiarities may exist even before the onset of disease (Fig. 3).

Although it is often difficult to find changes in the microvasculature due to large intersubject variability, AV channels in the parafoveal capillary network are disrupted even before the presence of any clinical signs ($P < 0.05$), and this change appears to precede measureable levels of capillary dropout as well as alterations to leukocyte flow. As such, AV channel tortuosity is the most promising candidate as an imaging biomarker for evaluating the efficacy of a therapeutic agent or as a tool for assessing the onset and progression of DR.

References

1. Wong TY, Cheung N, Tay WT, et al. Prevalence and risk factors for diabetic retinopathy: The Singapore Malay Eye Study. *Ophthalmology.* 2008;115:1869–1875.
2. Kwan AS, Barry C, McAllister IL, Constable I. Fluorescein angiography and adverse drug reactions revisited: the Lions eye experience. *Clini and Exp Ophthalmol.* 2006;34:33–38.
3. Alder VA, Su EN, Yu DY, Cringle SJ, Yu PK. Diabetic retinopathy: early functional changes. *Clin Exp Pharmacol Physiol.* 1997;24: 785–788.

4. Kim SY, Johnson MA, McLeod S, et al. Retinopathy in monkeys with spontaneous type 2 diabetes. *Invest Ophthalmol Visual Sci.* 2004;45:4543–4553.

5. Chambers R, Zweifach BW. Topography and function of the mesenteric capillary circulation. *Am J of Anatomy.* 1944;75:173–205.

6. Hasegawa T, Ravens JR, Toole JF. Precapillary arteriovenous anastomoses: "throughfare channels" in the brain. *Arch Neurol.* 1967;16:217–224.

7. Tam J, Tiruveedhula P, Roorda A. Characterization of single-file flow through human retinal parafoveal capillaries using an adaptive optics scanning laser ophthalmoscope. *Biomed Opt Express.* 2011;2:781–793.

8. Ludovico J, Bernardes R, Pires I, Figueria J, Lobo C, Cunha-Vaz J. Alterations of retinal capillary blood flow in preclinical retinopathy in subjects with type 2 diabetes. *Graefes Arch Clin Exp Ophthalmol.* 2003;241:181–186.

9. Arend O, Wolf S, Remky A, et al. Perifoveal microcirculation with non-insulin-dependent diabetes mellitus. *Graefes Arch Clin Exp Ophthalmol.* 1994;232:225–231.

10. Bresnick GH, Condit R, Syrjala S, Palta M, Groo A, Korth K. Abnormalities of the foveal avascular zone in diabetic retinopathy. *Arch Ophthalmol.* 1984;102:1286–1293.

11. Mansour AM, Schachat A, Bodiford G, Haymond R. Foveal avascular zone in diabetes mellitus. *Retina.* 1993;13:125–128.

12. Conrath J, Giorgi R, Raccah D, Ridings B. Foveal avascular zone in diabetic retinopathy: quantitative vs qualitative assessment. *Eye.* 2005;19:322–326.

13. Sander B, Larsen M, Engler C, Lund-Andersen H, Parving H-H. Early changes in diabetic retinopathy: capillary loss and blood-retina barrier permeability in relation to metabolic control. *Acta Ophthalmol.* 1994;72:553–559.

14. Hilmantel G, Applegate RA, Van Heuven WAJ, Stowers SP, Bradley A, Lee BL. Entoptic foveal avascular zone measurement and diabetic retinopathy. *Optom Vis Sci.* 1999;76:826–831.

15. Snodderly DM, Weinhaus RS, Choi JC. Neural-vascular relationships in central retina of macaque monkeys (Macaca fascicularis). *J Neurosci.* 1992;12:1169–1193.

16. Yu PK, Balaratnasingam C, Cringle SJ, McAllister IL, Provis J, Yu DY. Microstructure and network organisation of the microvasculature in the human macula. *Invest Ophthalmol Vis Sci.* 2010;51:6735–6743.

17. Michaelson IC, Campbell ACP. The anatomy of the finer retinal vessels. *Tr Ophth Soc U K.* 1940;60:71–112.

18. Tam J, Martin JA, Roorda A. Non-invasive visualization and analysis of parafoveal capillaries in humans. *Invest Ophthalmol Vis Sci.* 2010;51:1691–1698.

19. Tam J, Roorda A. Speed quantification and tracking of moving objects in adaptive optics scanning laser ophthalmoscopy. *J Biomed Opt.* 2011;16:036022.

20. Zhang Y, Poonja S, Roorda A. MEMS-based adaptive optics scanning laser ophthalmoscopy. *Opt Lett.* 2006;31:1268–1270.

21. Roorda A, Romero-Borja F, Donnelly III WJ, Queener H, Hebert TJ, Campbell MCW. Adaptive optics scanning laser ophthalmoscopy. *Opt Express.* 2002;10:405–412.

22. Garcia CR, Rivero ME, Bartsch DU, et al. Oral fluorescein angiography with the confocal scanning laser ophthalmoscope. *Ophthalmology.* 1999;106:1114–1118.

23. Li KY, Tiruveedhula P, Roorda A. Inter-subject variability of foveal cone photoreceptor density in relation to eye length. *Invest Ophthalmol Vis Sci.* 2010;51:6858–6867.

24. West SK, Klein R, Rodriguez J, et al. Diabetes and diabetic retinopathy in a Mexican-American population. *Diabetes Care.* 2001;24:1204–1209.

25. Hart WE, Goldbaum M, Cote B, Kube P, Nelson MR. Automated measurement of retinal vascular tortuosity. *Proc AMIA Annu Fall Symp.* 1997;459.

26. Kim SY, Johnson MA, McLeod S, Alexander T, Hansen BC, Lutty GA. Neutrophils are associated with capillary closure in spontaneously diabetic monkey retinas. *Diabetes.* 2005;54:1534–1542.

27. Chibber R, Ben-Mahmud BM, Chibber S, Kohner EM. Leukocytes in diabetic retinopathy. *Curr Diabetes Rev.* 2007;3:3–14.

28. Miyamoto K, Ogura Y. Pathogenic potential of leukocytes in diabetic retinopathy. *Semin Ophthalmol.* 1999;14:233–239.

29. Braun RD, Fisher TC, Meiselman HJ, Hatchell DL. Decreased deformability of polymorphonuclear leukocytes in diabetic cats. *Microcirculation.* 1996;3:271–278.

30. Ashton N. Studies of the retinal capillaries in relation to diabetic and other retinopathies. *Br J Ophthalmol.* 1963;47:521–538.

31. Kylstra JA, Wierzbicki T, Wolbarsht ML, Landers MB, Stefansson E. The relationship between retinal vessel tortuosity, diameter, and transmural pressure. *Graefes Arch Clin Exp Ophthalmol.* 1986;224:477–480.

32. Feke GT, Buzney SM, Ogasawara H, et al. Retinal circulatory abnormalities in type 1 diabetes. *Invest Ophthalmol Vis Sci.* 1994;35:2968–2975.

33. Bursell SE, Clermont AC, Kinsley BT, Simonson DC, Aiello LM, Wolpert HA. Retinal blood flow changes in patients with insulin-dependent diabetes mellitus and no diabetic retinopathy. *Invest Ophthalmol Vis Sci.* 1996;37:886–897.

34. Konno S, Feke GT, Yoshida A, Fujio N, Goger DG, Buzney SM. Retinal blood flow changes in type I diabetes: a long-term follow-up study. *Invest Ophthalmol Vis Sci.* 1996;37:1140–1148.

35. Kohner EM, Hamilton AMP, Saunders SJ, Sutcliffe BA, Bulpitt CJ. The retinal blood flow in diabetes. *Diabetologia.* 1975;11:27–33.

36. Cunha-Vaz J, Fonseca JR, de Abreu JRF, Lijma JJP. Studies on retinal blood flow, II: diabetic retinopathy. *Arch Ophthalmol.* 1978;96:809–811.

37. Patel V, Rassam S, Newsom R, Wick J, Kohner E. Retinal blood flow in diabetic retinopathy. *BMJ.* 1992;305:678–683.

38. Geyer O, Neudorfer M, Snir T, et al. Pulsatile ocular blood flow in diabetic retinopathy. *Acta Ophthalmol Scand.* 1999;77:522–525.

39. Savage HI, Hendrix JW, Peterson DC, Young H, Wilkinson CP. Differences in pulsatile ocular blood flow among three classifications of diabetic retinopathy. *Invest Ophthalmol Vis Sci.* 2004;45:4504–4509.

40. MacKinnon JR, O'Brien C, Swa K, Aspinall P, Butt Z, Cameron D. Pulsatile ocular blood flow in untreated diabetic retinopathy. *Acta Ophthalmol Scand.* 2009;75:661–664.

41. Schmid-Schonbein GW, Usami S, Skalak R, Chien S. The interaction of leukocytes and erythrocytes in capillary and postcapillary vessels. *Microvasc Res.* 1980;19:45–70.

42. Pécsvárády Z, Fisher TC, Darwin CH, et al. Decreased polymorphonuclear leukocyte deformability in NIDDM. *Diabetes Care.* 1994;17:57–63.

43. Klein R, Klein BEK, Moss SE, Davis MD, DeMets DL. The Wisconsin epidemiologic study of diabetic retinopathy, III: prevalence and risk of diabetic retinopathy when age at diagnosis is 30 or more years. *Arch Ophthalmol.* 1984;102:527–532.

44. Nelson DA, Krupsky S, Pollack A, et al. Special report: noninvasive multi-parameter functional optical imaging of the eye. *Ophthalmic Surg Lasers Imaging.* 2005;36:57–66.

45. Schmoll T, Singh ASG, Blatter C, et al. Imaging of the parafoveal capillary network and its integrity analysis using fractal dimension. *Biomed Opt Express.* 2011;2:1159–1168.

46. Kim DY, Fingler J, Werner JS, Schwartz DM, Fraser SE, Zawadzki RJ. Visualization of human retinal micro-capillaries with phase contrast high-speed optical coherence tomography. *Proc of SPIE.* 2011;7889:78890H–78896H.